Models of Low Mass Stars in the Local Solar Neighborhood and in Globular Clusters

A Thesis Proposal

Submitted to the Faculty
in partial fulfillment of the requirements for the
degree of

Doctor of Philosophy

in

Physics and Astronomy

by

Thomas M. Boudreaux

DARTMOUTH COLLEGE
Hanover, NH
May 10, 2022

The Examining Committee:

Dr. Brian Chaboyer

Dr. Elisabeth E. Newton

Dr. Aaron Dotter

Draft version April 12, 2022
Typeset using LaTeX **manuscript** style in AASTeX62

ABSTRACT

The equations of stellar structure have proven astonishingly predictive when describing stars interior structures. In their most basic form they constitute 4 ordinary, first-order, differential equations. However, they are not on their own well enough constrained to solve. In addition to the four ODEs, an equation of state, thermal conductivities, nuclear reaction rates, and opacities are all required when modeling a star. Some of these additional constraints can be computed on the fly; however, as yet there is no effective way to compute opacities at run time. Rather, stellar structure programs use pre-tabulated opacities over a range of temperatures, densities, and chemical compositions. The Dartmouth Stellar Evolution Program (DSEP) has used OPAL opacities for the last decade and a half; however, there are now more up to date elemental opacity tables from OPLIB. Moreover, OPAL opacities can no longer be reliably generated for different chemical compositions. Here we present an overview of how we update DSEP to use opacities from OPLIB in addition to preliminary results from two studies making use of these updated opacities.

1. INTRODUCTION

Over the last half of the 19th and first decade of the 20th centuries Lane, Ritter, and Emden codified the earliest mathematical model of stellar structure, the polytrope (Equation 1), in *Gaskugeln* (Gas Balls) (Emden 1907).

$$\frac{d}{d\xi}\left(\xi^2\frac{d\theta}{d\xi}\right) = -\xi^2\theta^n \tag{1}$$

Where ξ and θ are dimensionless parameterizations of radius and temperature respectively, and n is known as the polytropic index. Despite this early work, it wasn't until the late 1930s and early 1940s that the full set of equations needed to describe the structure of a steady state, radially-symmetric, star (known as the equations of stellar structure) began to take shape as proton-proton chains and

the Carbon-Nitrogen-Oxygen cycle were, for the first time, seriously considered as energy generation mechanisms (Cowling 1966). Since then, and especially with the proliferation of computers in astronomy, the equations of stellar structure have proven themselves an incredibly predictive set of models.

There are currently many stellar structure codes (e.g. Dotter et al. 2008; Kovetz et al. 2009; Paxton et al. 2011) which integrate the equations of stellar structure — in addition to equations of state and lattices of nuclear reaction rates — over time to track the evolution of an individual star. The Dartmouth Stellar Evolution Program (DSEP) (Chaboyer et al. 2001; Bjork & Chaboyer 2006; Dotter et al. 2008) is one such, well tested, stellar evolution program.

Here we propose to model low-mass stars in both the local solar neighborhood and in globular clusters using DSEP. This work will primarily extend our understanding of stellar physics in two areas: the effects of chemically self-consistency on stellar models and time evolution of the core-convective instabilities which ultimatly are belived to result in the observed paucity of stars at a Gaia G magnitude of ∼10. [NEED CITATIONS IN THIS PARAGRAPH]

Low mass stars form an important component of the stellar population, with stars less than [MASS HERE] making up more than 70% of stars in the galaxy [CITE]. Moreover, due to their long lives, low-mass stars provide essential constraints on ages of various stellar populations [CITE]. In globular clusters, where all stars are coeval to one of a limited number of populations, low mass stars provide the vast majority of constraints when fitting ischrones [CITE]. Additionally, stars around the fully-convective transition mass show age-dependent core-convective instabilities [CITE].

1.1. *Globular Clusters*

Globular clusters in the local universe are primarly composed of old and consequently low-mass stars. For decades, prevaling thought had it globular clusters were composed of a single stellar population born from a preisten interstellar medium. This was supported by visibly tight main sequences and clear main sequence turn offs in optical CMDs (Figure 1, Sandage 1953). These

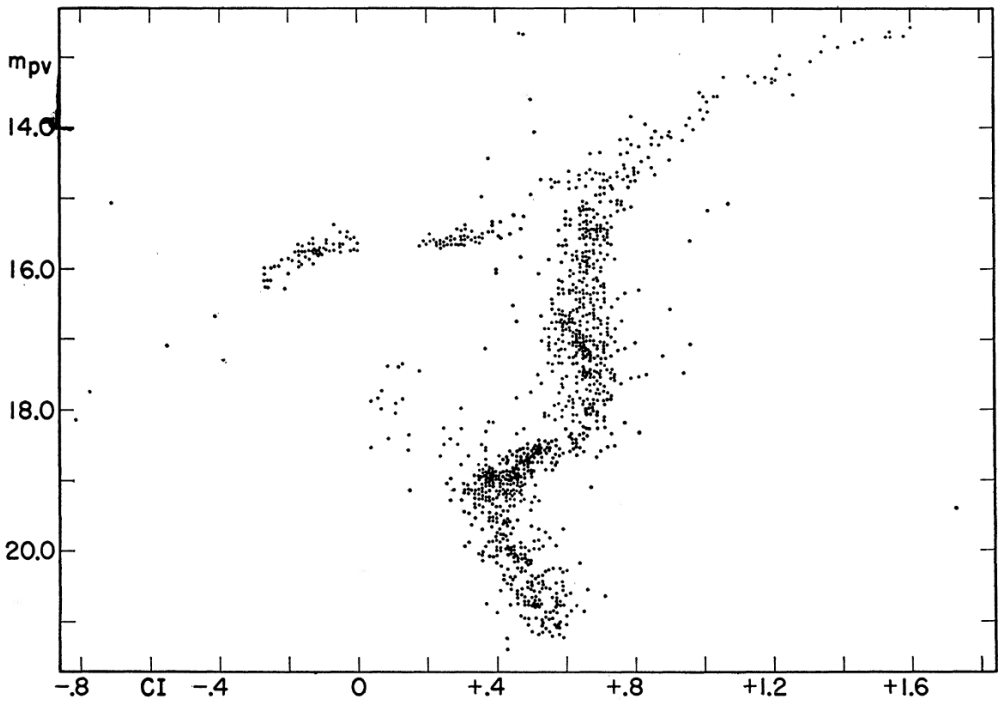

Figure 1. m_{pg} - m_{pv} color-magnitude diagram for the globular cluster M3.

early studies either did not handel or had very large photometric uncertanties and therefore they were unable to discriminate beteween CMD features with small separations,

[SOMETHING ABOUT EARLY SPECTROSCOPIC INDICATIONS OF MPs]

With the presicion photometric measurements, degenerecies between noise and intrinsic scatter were broken and it became clear that globular clusters are almost universally composed of multiple stellar populations (MPs). [GRAB SOME TEXT FROM THE NGC 2808 SECTION FOR HERE].

1.2. *Local Solar Neighborhood*

Jao et al. (2018) discovered a novel feature in the Gaia Gp-Rp color-magnitude diagram. Around $M_G = 10$ there is an approximatly 17% decreas in stellar density of the volume complete sample of stars Jao et al. considered. Subsequently, this has become known as either the Jao Gap, or Gaia M dwarf Gap. Section **??** will go into more detail regarding the physics belived to underpin this feature; however, in brief convective instabilities in the core are belived to form for stars straddeling

the fully convective transition mass. These instabilities result in stars preferentially falling to either side of the gap location.

Stellar modeling has been sucsessful in reproducing the Jap Gap and, with these models, we have begun to constrain parameters which constrain gap location. For example, it is now well documented that a stars metallicity can affect the gap color by up to [HOW MUCH DID GREG FIND/CHECK FOR OTHER PAPERS ON THIS].

Initial testting which we have done using DSEP along with work by [PAPER] also indicated the Jao Gap's color sensitivity to age. We observe that as models age the Jao Gap moves [DIRECTION OF MOVMENT IN MAG AND COLOR SPACE]. Sections **??** and **??** of this proposal lay out a plan to use this observed age-dependence to date low-mass stars in the local-solar neighborhood.

1.3. *OPAL (move?)*

The OPAL opacity tables in particular are very widely used by current generation stellar evolution programs (in addition to current generation stellar model and isochrone grids). However, they are no longer the most up date elemental opacities. Moreover, the generation mechanism for these tables, a webform, is no longer reliably online. Consequently, it makes sense to transition to more modern opacity tables with a more stable generation mechanism.

Here we will present work transitioning DSEP from OPAL opacities to opacities based on measurements from Los Alamos national Labs T-1 group (OPLIB Colgan et al. 2016). Moreover, we will present two projects which are in large part reliant on these updated opacities. For the first project we investigate the affects of chemically self consistent modeling of multiple populations within the globular cluster NGC 2808, and for the second project we present the effects of the OPLIB opacities on the location of the recently discovered Gaia M-dwarf gap.

This paper is organized as follows. In Section **??** we outline some basic information about OPLIB opacities, how we query them, and how we modify them to work with DSEP. In Section **??** we discuss scientific background of the first project along with the current work done towards its goal.

Finally, in Section **??** we present our findings on the effects of OPLIB opacities on the location of the Gaia M-dwarf gap.

2. DSEP

DSEP solves the equations of stellar structure using the Henyey method (Henyey et al. 1964). This is a relaxation technique making use of a Newton–Raphson root finder and therefore requires some initial guess to relax towards a solution. This guess will be either some initial, polytropic, model or the solution from the previous timestep. In order to evolve a model through time DSEP alternates between solving for reaction rates and the structure equations. At some temperature and pressure from the solution to the structure equations DSEP finds the energy generation rate due to proton-proton chains, the CNO cycle, and the tripe-alpha process from known nuclear cross sections. These reaction rates yield both photon and neutrino luminosities as well as chemical changes over some small time step. Thermodynamic variables are calculated using an equation of state routine which is dependent on the initial model mass. All the updated physical quantities (pressure, luminosity, mean molecular mass, temperature) are then used to solve the structure equations again. This process of using a solution to the structure equations to calculate reaction rates which then inform the next structure solution continues until DSEP can no longer find a solution. This can happen as the stellar structure equations are extremely stiff. In addition, for finite radial mesh sizes, discontinuities can occur.

While other stellar evolution programs, such as the widely used Modules for Experimentation in Stellar Astrophysics (MESA) (Paxton et al. 2011), consider a more complex handling of nuclear reaction rate calculations, and are consequently more applicable to a wider range of spectral classes than DSEP, DSEP has certain advantages over these other programs that make it well suited for certain tasks, such as low-mass modeling. For one, DSEP generally can evolve models much more rapidly than MESA and has a smaller memory footprint while doing it. This execution time difference is largely due to the fact that DSEP makes some simplifying assumptions due to its focus only on models with initial masses between 0.1 and 5 $M_\odot$ compared to MESA's more general

approach. Moreover, MESA elects to take a very careful handling of numeric uncertainty, going so far as to guarantee byte-to-byte similarity of the same model run on different architectures (Paxton et al. 2011). DSEP on the other hand makes no such guarantee. Rather, models evolved using DSEP will be accurate down to some arbitrary, user controllable, tolerance but beyond that point may vary from one computer to another. Despite this trade off in generality and precision, the current grid of isochrones generated by DSEP (Dotter et al. 2008), has been heavily cited since its initial release in 2008, proving that there is a place for a code as specific as DSEP.

As DSEP pushes a star along its evolutionary track the radiative opacity must be known for a wide range of temperatures, pressures, and compositions. Specifically, opacity is a key parameter in the equation of energy transport. With current computational tools it's infeasible to compute opacities on the fly; rather, Rossland Mean opacity (κ_R) for individual elements must be pre-tabulated over a wide range of temperatures and densities. These opacities can then be somewhat arbitrarily mixed together and interpolated to form opacity lookup-tables. Multiple groups have preformed these calculations and subsequently made tables available to the wider community, these include the Opacity Project (OP Seaton et al. 1994), Laurence Livermore National Labs OPAL opacity tables (Iglesias & Rogers 1996), and Los Alamos National Labs OPLIB opacity tables (Colgan et al. 2016).

3. THESIS

The thesis here proposed will be split into 5 chapters. Each chapter will consist of work focusing on models low mass stars.

3.1. *Jao Gap & Updated High Temperature Opacities*

Due to initial mass requirements of the molecular clouds which collapse to form stars, star formation is strongly biased towards lower mass, later spectral class, stars when compared to higher mass stars. Partly as a result of this bias and partly as a result of their extremely long main-sequence lifetimes, M-dwarfs make up approximately 70 percent of all stars in the galaxy. Moreover, some planet search campaigns have focused on M-dwarfs due to the relative ease of detecting small plan-

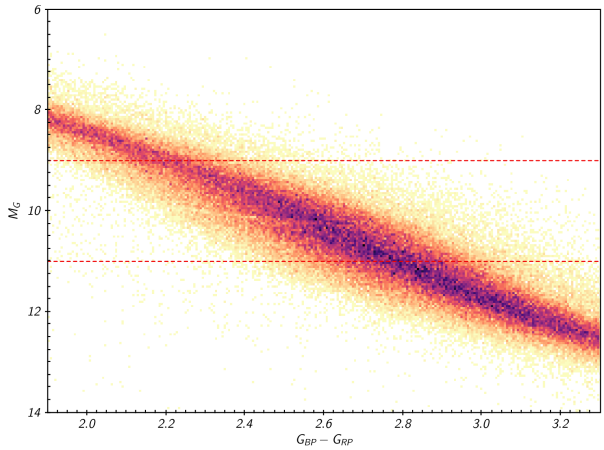

Figure 2. Figure 1 from Jao et al. (2018) showing the so called "Jao Gap" at $M_G \approx 10$

ets in their habitable zones (e.g. Nutzman & Charbonneau 2008). M-dwarfs then represent both a key component of the galactic stellar population as well as the possible set of stars which may host habitable exo-planets. Given this key location M-dwarfs occupy in modern astronomy it is important to have a thorough understanding of their structure and evolution.

3.1.1. *Observations and Instability*

Gaia Data Release 2 (DR2) revealed a previously unknown structure in in the $G_{\rm BP} - G_{\rm RP}$, M_G color-magnitude diagram (Figure 2) corresponding to stars with a mass near that where a star transitions from fully convective to having both convective and radiative regions within (the fully convective transition mass) (Jao et al. 2018). The so called Gaia M-dwarf gap, or Jao gap, represents a decrease in luminosity and commensurately a decrease in stellar density — by approximately 17% — over this mass range. Jao et al. (2018); Baraffe & Chabrier (2018) suggest that this density deficiency is due to stars between a mass of 0.3 to 0.35 $M_\odot$ transitioning into full convectivity.

A theoretical explanation for such a density deficiency comes from van Saders & Pinsonneault (2012), who propose that directly above the transition mass between a star with a radiative core and convective envelope and a fully convective star, due to asymmetric production and destruction of He^3 during the proton-proton I chain (ppI), periodic luminosity variations can be induced. This process is known as convective-kissing instability. Take for example a star with a mass right on the

fully convective transition. Such a star will descent the pre-MS with a radiative core; however, as the star reaches the zero age main sequence (ZAMS) and as the core temperature exceeds 7×10^6 K, enough energy will be produced by the ppI chain that the core becomes convective. At this point the star exists with both a convective core and envelope, in addition to a thin, radiative, layer separating the two. At this Point asymmetries in ppI affect the evolution of the stars convective core.

The proton-proton I chain constitutes three reactions

1. $p + p \longrightarrow d + e^+ + \nu_e$
2. $p + d \longrightarrow {}^3\mathrm{He} + \gamma$
3. ${}^3\mathrm{He} + {}^3\mathrm{He} \longrightarrow {}^3\mathrm{He} + 2p$

Because reaction 3 of ppI consumes ^{3}He at a slower rate than it is produced by reaction 2, ^{3}He abundance increases in the core increasing energy generation. The core convective zone will therefore expand as more of the star becomes unstable to convection. This expansion will continue until the core connects with the convective envelope. At this point convective mixing can transport material throughout the entire radius of the star and the high concentration of ^{3}He will rapidly diffuse outward, away from the core, again decreasing energy generation as reaction 3 slows Down. Ultimately, this leads to the convective region around the core pulling back away from the convective envelope, leaving in place the radiative transition zone, at which point ^{3}He concentrations build up in the until it once again expands to meet the envelope. This process repeats until chemical equilibrium is reached throughout the star and the core can sustain high enough nuclear reaction rates to maintain contact with the envelope, resulting in a fully convective star.

3.1.2. *Modeling the Gap*

Since the identification of the Gaia M-dwarf gap, stellar modeling has been conducted to better constrain its location, effects, and exact cause (e.g. Mansfield & Kroupa 2021; Feiden et al. 2021). When modeling the gap manifests as a discontinuity in the mass-luminosity relation. However, all

modeling of the gap has been done using GS98 OPAL high-temperature opacities. This presents similar issues to the use of these tables when modeling multiple populations in GCs; namely, OPAL tables are no longer the most up to date in their component opacities .

Mansfield & Kroupa (2021) and Feiden et al. (2021) identify that the gap's mass location is correlated with model metallicity — the mass-luminosity discontinuity in lower metallicity models being at a commensurately lower mass. Feiden et al. (2021) suggests this dependence is due to the steep relation of the radiative temperature gradient, ∇_{rad}, on temperature and in turn, on stellar mass.

$$\nabla_{rad} \propto \frac{L\kappa}{T^4} \tag{2}$$

As metallicity decreases so does opacity, which, by Equation 2, dramatically lowers the temperature where radiation will dominate energy transport (Chabrier & Baraffe 1997). Since main sequence stars are virialized the core temperature is proportional to the core density and total mass (Equation 3). Therefore, if the core temperature where convective-kissing instability is expected decreases with metallicity, so to will the mass of stars which experience such instabilities.

$$T_c \propto \rho_c M^2 \tag{3}$$

3.1.3. *Consistently Modeling the Gap*

In order to address the two main issues with using OPAL opacity tables we use our OPLIB opacity table web scraper to generate a set of tables that consistently model lower metallicities. Specifically, we generate tables for $Z_\odot = 0.017$, $Z = 0.01$, $Z = 0.001$, and $Z = 0.0001$. Compositions are derived from the GS98 solar composition, with the mass fractions between metals remaining constant, and only the total metal mass fraction is allowed to vary. Moreover, Helium mass fraction is held constant as extra mass from the reduced metallicity is put into additional Hydrogen.

For each metallicity 101, uniformly spaced, models from 0.3 to 0.5 $M_\odot$ (spacing of 0.001 $M_\odot$) are evolve with both the GS98 OPAL opacity table and OPLIB tables, hereafter these are the "coarse"

$Z =$	$Z_\odot$	0.01	0.001	0.0001
OPAL	0.3803 - 0.384	0.3583 - 0.3631	0.34 - 0.3448	0.362 - 0.3663
OPLIB	0.374 - 0.3767	0.3526 - 0.3567	0.3358 - 0.3406	0.3577 - 0.3621

Table 1. Mass ranges for the discontinuity in OPAL and OPLIB models. Masses are given in solar masses.

models. For each set of coarse models the discontinuity in the mass-luminosity relation is identified at an age of 7 Gyr (Figures **??** & **??** shows a characteristic example).

Immediately, the difference in mass where the discontinuity manifests is clear. For each metallicity the discontinuity in the OPLIB models is approximately one one-hundredth of a solar mass lower than the discontinuity in the OPAL models. We can validate that this discontinuity is indeed correlated with the convective transition mass; Figure **??** shows an example of the model forming radiative zones at approximately the same masses where the discontinuity in the mass-luminosity function exists.

At this resolution only a few models exist within the mass range of the discontinuity. In order to better constrain its location we run a series of "fine" models, with a mass step of 0.0001 $M_\odot$ and ranging from where the mass derivative first exceeds two sigma away from the mean derivative value up to the mass where it last exceeds two sigma away from the mean. A characteristic fine mass-luminosity relation is shown in Figure **??**.

Using the fine models we identify the location of the discontinuity in the same manner as before, results of this are presented in Table 1. Of note with the mass ranges we measure for the discontinuity is that are generally not in agreement with those measured in Mansfield & Kroupa (2021). However, the luminosity difference from over the gap ($\approx 0.1 mag$) is similar to both the observational difference and that reported in Mansfield & Kroupa (2021). Currently, it is not clear why our mass range is not in agreement with the Mansfield & Kroupa (2021) mass range and further investigation is therefore needed.

3.2. *Jao Gap Ageing - 1*

Following the integration of updated high temperature opacities detiled in §3.1 we will investigate using the Jao-Gap color to age the local solar neighboorhood.

Preilimiary modeling we have done, along with past literature [CITE] demonstrates that the Jao Gap is expected to migrate along the main sequence as a population of stars age. Stellar populations younger than $\sim 3Gyr$ do not show a gap. Once the gap forms it will migrate towrds brighter portions of the CMD.

For this proposal we do not preform any rigorous statistical testing of whether the differences in theoretical Jao Gap location could be discrimated between in observational data; instead, choosing to save that element of the research for thesis work proper. However, we do preform a qualitative test of the visual distinguisability of the Jao Gap location for two sample sizes — 500 and 1000 stars (Figure 3).

$$\xi(m) = \xi_0 \left(\frac{m}{M_\odot} \right)^{-2.68 \pm 0.09} \tag{4}$$

We evolve models over an extremely finley sampled mass grid centered at the theoretical Jao Gap location for a GS98 solar composition population of stars. We then adopt the (Sollima 2019) IMF between 0.1 and 1 $M_\odot$ (Equation 4) to sample these evolved models. Model surface gravities, effective temperatures, and luminosities are transformed into Gaia magnitudes using bolometric correction tables provided by ESA[1]. Uncertainty is injected by first transforming G, BP, and RP flux and flux uncertaninty measurments for all stars Gaia observed within 10pc to magnitude and magnitude uncertaninties. Flux errors do not transform into symetric magnitude errors; however, for small uncertaninties the transformation may be approximated as symetric (Equations 5 & 6).

$$M_x = -2.5 \log_{10}(I_x) + ZP_x \tag{5}$$

$$\sigma_x = \left(\frac{1.086 \sigma_{I_x}}{I_x} \right)^2 + ZP^2_{\sigma_{I_x}} \tag{6}$$

[1] FOOTNOTE HERE

Where x is the band of interest, I_x is the measured flux in that band, and ZP_x is the zero point offset in `VEGAMAG`. Following this transformation, we fit a second-order polynominal to the magnitude error v.s. magnitude for each band. This polynominal gives an approximation of the mean uncertaninty for a given magnitude. For each point sampled from the IMF and set of evolved models we add a sample from a normal distributions centered at 0 and with a standard deviation equal to the evaluation of the optimized quadradic at that points magnitude.

Figure 3 Panels A and B show (1 Gyr) do not show any visible Jao Gap; whereas, Panels C, D, E, and F all do. Moreover, the location of the Gap visible shiftes to lower magnitudes from 3 Gyr to 6 Gyrs. Note that this shift is apparent in CMDs with both 1000s stars and those with 500 stars. In fact, visually, this shift is clear with CMDs containing as few as 100 stars within this mass range. Obviously, a simple visual identification is prone to confirmation bias; however, we belive that these results are sufficent to warrent a future, more rigorus, study.

Models predict that the location of the Jap Gap will shift with population age [CITATION]; in fact, we see this behavior, gap colors reddening as populations age, in populations evolved with DSEP [FIGURE] which span the mass range of the gap.

[DETAILS ON KINEMATIC AGEING]

We propose to model a population of stars of various ages and mettalicities sampled from the local stellar neighboorhood. Each of these stars will be assigned kinematics — again sampled from empirical distributions. We will then extract kinematically derived ages from this population and use these to segregate stars into rough age bins. Finally, we will measure if difference in Jao gap locations are statistically distinquishable between these rough age bins.

3.3. *Jao Gap Ageing - 2*

Where the project laied out in §3.2 study the feasibility of using the Jao Gap to date stellar populations; this project will apply this tequnique to observational data. Specifically, we measure the Jao Gap location in populations seperated by gyro-kinematic dataing in the solar neighboorhood.

3.4. *NGC 2808*

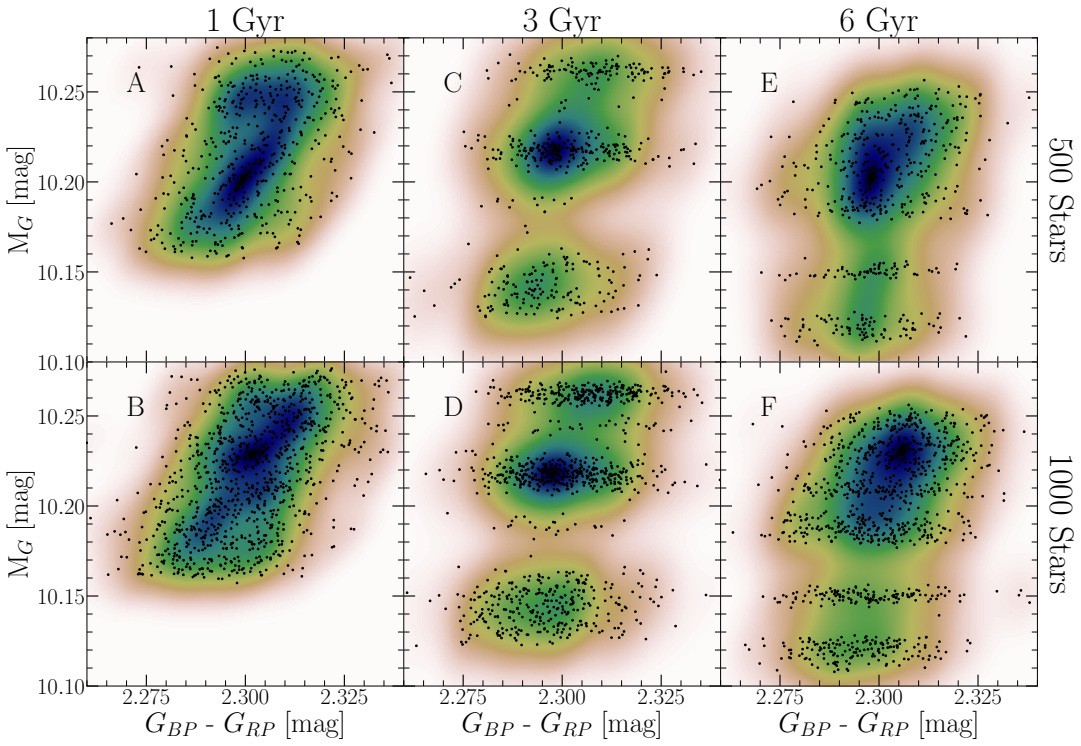

Figure 3. Populations synthetis results for a mass range surrounding the theoretical location of the Jao Gap at 3 population ages and with different sample sizes. The superimposed color map is derived from a gaussian kernel-density-estimation run on the displayed points. This is included to better illustrate the gap location.

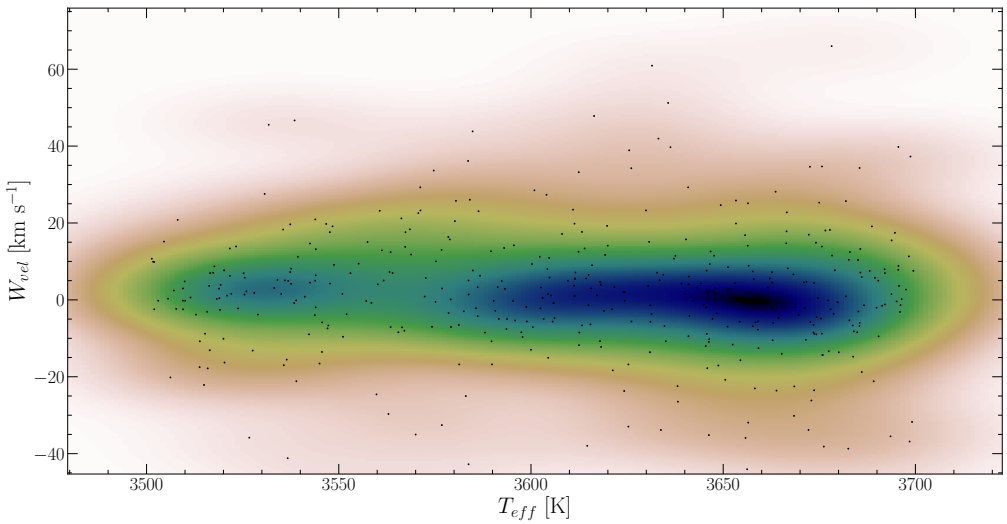

Figure 4. Kernel Density Estimation function of the gyro-kinematically infered velocity vs. effetive temperature. This sample is selected from Lu et al. (2021) and cut between $T_{eff} < 3800$ K and $T_{eff} > 3500$ K.

Globular clusters (GC, Herschel 1814) are among the oldest groupings of stars in the Universe, with typical ages greater than 10 Gyr. They are characterized by their compact size — typical half-light radius < 10 pc but up to 10s of pc — and high surface brightness — $M_V \sim -7$. Traditionally, GCs were believed to contain a single stellar population, much like open clusters. However, chemical inhomogeneities in GCs have been known about since the early 1970s (e.g. Osborn 1971) and by the late 1980s multiple clusters were known which exhibited features in their CMDs consistent with either bimodal or multimodal stellar populations (e.g. Norris 1987).

Whereas, people have have often tried to categorized objects as GCs by making cuts along half-light radius, density, and surface brightness profile, in fact many objects which are generally thought of as GCs don't cleanly fit into these cuts. Consequently, Carretta et al. (2010) proposed a definition of GC based on observed chemical inhomogeneities in their stellar populations. The modern understanding of GCs then is not simply one of a dense cluster of stars which may have chemical inhomogeneities and multiple populations; rather, it is one where those chemical inhomogeneities and multiple populations themselves are the defining element of a GC.

Variations in observed abundances were initially attributed to evolutionary mixing (Denisenkov & Denisenkova 1990). However, enhanced abundances are still observed in scarcely evolved main sequence stars, ruling out evolutionary mixing as the primary mechanism (Gratton et al. 2004; Briley et al. 2004). Moreover, mixing of a degree high enough to explain the observed anomaly in cyanogen abundances would result in extended lifetimes and a broadened main sequence turn off region in the CMD of ancient GCs, which is not observationally supported. More recently, precision Hubble photometry revealed that almost every cluster in orbit of the milky way comprises multiple main sequences (Piotto et al. 2007; Roh et al. 2011; Milone et al. 2012) (MMP) as opposed to a single stellar population (SP).

Single stellar populations had been assumed due to spectroscopically uniform iron abundances (Gratton et al. 2012) and very narrow principal sequences (Stetson & Harris 1988), both of which are indicative of a single stellar population. The first conclusive evidence for MMPs came with Hubble Space Telescope (HST) high precision crowded field photometry in which three distinct

main sequences in NGC 2808 were identified (Piotto et al. 2007). Since this discovery, split main sequences have been found in nearly all Milky Way globular clusters studied by HST (Anderson et al. 2009; Milone et al. 2012). Split stellar populations are believed to be due to enhanced helium abundances in the stellar populations formed after the primordial population of stars (D'Antona et al. 2005; Piotto et al. 2007). When compared to primordial helium mass fractions (Y) of $Y \sim 0.25$ (Collaboration et al. 2016) or solar helium abundances $Y \sim 0.27$ (Vinyoles et al. 2017) these populations have mass fractions as high as $Y \sim 0.4$. Helium enhancement is strongly suspected to be the result of an earlier, more massive population dying off, enriching the interstellar medium (Gratton et al. 2001, 2004, 2012). The primary open question then is not why some populations are enhanced in helium; rather, it is to what extent they are enhanced.

Due to the relatively high and tight temperature range of partial ionization for helium it cannot be observed in globular clusters; consequently, the evidence for these enhanced helium abundances originates from comparison of theoretical stellar isochrones to the observed color magnitude diagrams of globular clusters. None of the isochrones used to date in these comparison have been generated from models with self consistent chemistries.

3.5. *Population Opacities*

Given the relative historic difficulty in generating new opacity tables, stellar models have tended to use opacity tables whos range of compositions is derived from simple rescaling of the some solar composition. Here we use our OPLIB web scraper to generate opacity tables with compositions specific to each population in NGC 2808.

These population have been studied in depth by Feiden and their chemical compositions were determined in Milone et al. (2015) (see Table 2 in that paper). While we cannot currently make fully self-consistent models due to still ongoing atmospheric modeling, we can make a first pass investigation of the affect of OPLIB opacities (Figure 5). Note how the models generated using OPLIB opacity tables have a systematically lower luminosity. Recall, that this is consistent with the overall lower opacities of the OPLIB tables.

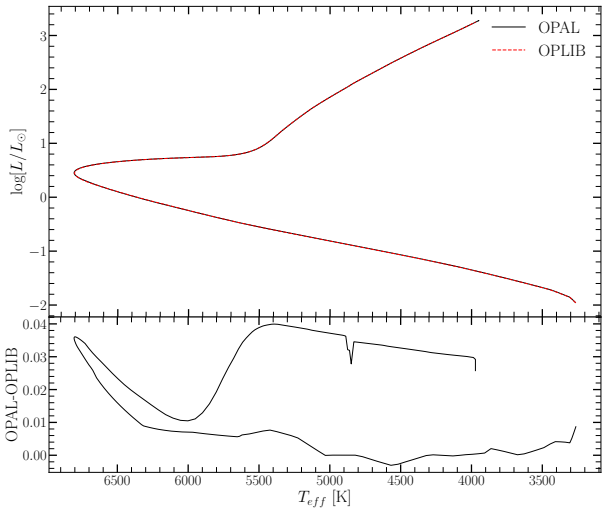

Figure 5. 10 Gyr & Y=0.33 isochrones for models generated with OPAL and OPLIB opacities tables (top). Residuals between isochrones (bottom).

3.6. *Additional Consistency*

The lack of self consistency presents problems at other stages of stellar evolution codes. Perhaps most importantly, where the interior of a stellar model meets the atmosphere. Atmospheric models such as a grey (Eddington 1916), Krishna Swamy (Krishna Swamy 1966), or Phoenix (Husser et al. 2013) model atmosphere provide one pressure boundary conditions to solve the two-point boundary value problem that is the equations of stellar structure. Once again however, models tend to use atmospheres with non consistent chemistries. Therefore, one key element of NGC 2808 modeling is the incorporation of new atmospheric models, generated from the MARCS grid of model atmospheres (Plez 2008), which match interior elemental abundances. Members of our collaboration are currently working on such atmospheric modeling.

Finally, The isochrones used to infer the degree of helium enhancements assume that convection operates in the same manner in metal-poor stars as it does in the Sun. However, observations from *Kepler* of metal-poor red giants (Bonaca et al. 2012; Tayar et al. 2017), in concert with interferometric radius determination of the metal-poor sub-giant HD 140283 (Creevey et al. 2015), have shown that the efficiency of convection changes with iron content. We will additionally modify DSEP to capture this variation in convective efficiency. While we wait for atmospheric modeling to

be completed it makes sense to investigate other locations where opacity differences on the order of 5% may affect results."s

3.7. *47 Tuc & NGC 6752*

In addition to NGC 2808, Feiden has generated MARCS atmospheric models for the clusters NGC 6752 and 47 Tuc. We will conduct the same, self-consistent, modeling for these clusters as we do for NGC 2808.

4. THESIS TIMELINE

We propose a thesis in five parts. Hereafter, the papers which will form the chapters of the thesis will be refered to P1, P2, P3, P4, and P5. These are enumerate in chronological order of submission.

The first paper, P1, detailing work already done to update DSEP to OPLIB opacity tables and the affects those new opacity tables have on the Jao Gap location will be submited in the Summer of 2022. The primary outstanding work for P1 is to run population synthetis models as, observationally, the Jao Gap is observed in populations of stars.

P2 covering self consistent modeling of NGC 2808, will be submited sometime between the start of the fall 2022 term and the spring 2023 term. Per Section **??** much of the background work for this paper has been completed and we are currently ramping up modeling efforts now that we have atmospheric models in hand. P4, consistent modeling of both 47 Tuc and NGC 6752 will follow directly from this work. Given P4's similarity to P2 we anticipate it will only take three terms to submit, with an expected submission term of summer 2023.

P3 will be submitted in the spring of 2023. This paper will focus on modeling populations of low mass stars in the local solar neighborhood in order to determin if the location of the Jao Gap in the CMD may be used to date these populations. Work on this paper has not yet begun. Finally, P5 will follow up on the theoretical work from the P3; gathering archival photometric data from low-mass stars in the local solar neighborhood and comparing Jao Gap derived ages to ages derived from the age-velocity-dispersion relation.

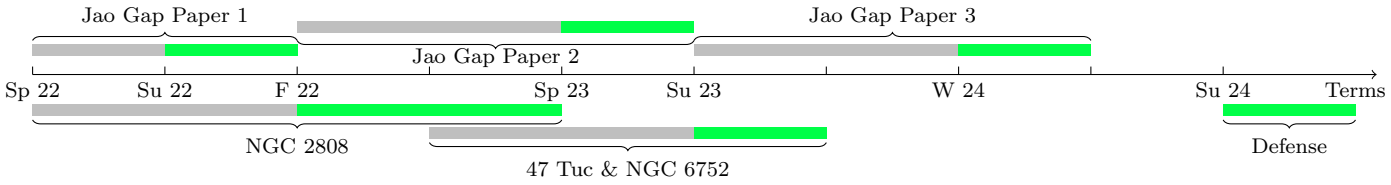

Figure 6. Proposed timeline for thesis work. Terms where a paper is expected to be submited are marked with green, terms where work on a project is intended to take place are marked in grey.

These five papers, in addition to an introductory chapter, will comprise a thesis to be defended sometime in the Summer 2024 term.

This research has made use of NASA's astrophysical data system (ADS). We acknowledge the support of an NASA grant (No. 80NSSC18K0634). Additionally, we would like to thank James Colgan for his assistance with the OPLIB opacity tables. We would like to thank Aaron Dotter, and Elisabeth Newton for their assistance. Finally, we thank our colleagues and peers in for their continuing and appreciated support.

REFERENCES

Anderson, J., Piotto, G., King, I., Bedin, L., & Guhathakurta, P. 2009, The Astrophysical Journal Letters, 697, L58

Baraffe, I., & Chabrier, G. 2018, A&A, 619, A177, doi: 10.1051/0004-6361/201834062

Bjork, S. R., & Chaboyer, B. 2006, ApJ, 641, 1102, doi: 10.1086/500505

Bonaca, A., Tanner, J. D., Basu, S., et al. 2012, The Astrophysical Journal Letters, 755, L12, doi: 10.1088/2041-8205/755/1/L12

Briley, M. M., Cohen, J. G., & Stetson, P. B. 2004, The Astronomical Journal, 127, 1579

Carretta, E., Bragaglia, A., Gratton, R. G., et al. 2010, Astronomy & Astrophysics, 516, A55

Chaboyer, B., Fenton, W. H., Nelan, J. E., Patnaude, D. J., & Simon, F. E. 2001, ApJ, 562, 521, doi: 10.1086/323872

Chabrier, G., & Baraffe, I. 1997, A&A, 327, 1039. https://arxiv.org/abs/astro-ph/9704118

Colgan, J., Kilcrease, D. P., Magee, N. H., et al. 2016, in APS Meeting Abstracts, Vol. 2016, APS Division of Atomic, Molecular and Optical Physics Meeting Abstracts, D1.008

Collaboration, P., et al. 2016, XIII. Cosmological parameters

Cowling, T. G. 1966, QJRAS, 7, 121

Creevey, O., Thévenin, F., Berio, P., et al. 2015, Astronomy & Astrophysics, 575, A26

Denisenkov, P. A., & Denisenkova, S. N. 1990, Soviet Astronomy Letters, 16, 275

Dotter, A., Chaboyer, B., Jevremović, D., et al. 2008, The Astrophysical Journal Supplement Series, 178, 89

D'Antona, F., Bellazzini, M., Caloi, V., et al. 2005, The Astrophysical Journal, 631, 868

Eddington, A. S. 1916, MNRAS, 77, 16, doi: 10.1093/mnras/77.1.16

Emden, R. 1907, Gaskugeln

Feiden, G. A., Skidmore, K., & Jao, W.-C. 2021, ApJ, 907, 53, doi: 10.3847/1538-4357/abcc03

Gratton, R., Sneden, C., & Carretta, E. 2004, ARA&A, 42, 385, doi: 10.1146/annurev.astro.42.053102.133945

Gratton, R. G., Carretta, E., & Bragaglia, A. 2012, Astronomy and Astrophysics Reviews, 20, 50, doi: 10.1007/s00159-012-0050-3

Gratton, R. G., Bonifacio, P., Bragaglia, A., et al. 2001, A&A, 369, 87, doi: 10.1051/0004-6361:20010144

Henyey, L. G., Forbes, J. E., & Gould, N. L. 1964, ApJ, 139, 306, doi: 10.1086/147754

Herschel, W. 1814, Philosophical Transactions of the Royal Society of London, 248

Husser, T. O., Wende-von Berg, S., Dreizler, S., et al. 2013, A&A, 553, A6, doi: 10.1051/0004-6361/201219058

Iglesias, C. A., & Rogers, F. J. 1996, ApJ, 464, 943, doi: 10.1086/177381

Jao, W.-C., Henry, T. J., Gies, D. R., & Hambly, N. C. 2018, ApJL, 861, L11, doi: 10.3847/2041-8213/aacdf6

Kovetz, A., Yaron, O., & Prialnik, D. 2009, MNRAS, 395, 1857, doi: 10.1111/j.1365-2966.2009.14670.x

Krishna Swamy, K. S. 1966, ApJ, 145, 174, doi: 10.1086/148752

Lu, Y. L., Angus, R., Curtis, J. L., David, T. J., & Kiman, R. 2021, AJ, 161, 189, doi: 10.3847/1538-3881/abe4d6

Mansfield, S., & Kroupa, P. 2021, A&A, 650, A184, doi: 10.1051/0004-6361/202140536

Milone, A., Marino, A., Piotto, G., et al. 2012, The Astrophysical Journal, 745, 27

Milone, A. P., Piotto, G., Bedin, L. R., et al. 2012, ApJ, 744, 58, doi: 10.1088/0004-637X/744/1/58

Milone, A. P., Marino, A. F., Piotto, G., et al. 2015, ApJ, 808, 51, doi: 10.1088/0004-637X/808/1/51

Norris, J. 1987, The Astrophysical Journal, 313, L65

Nutzman, P., & Charbonneau, D. 2008, PASP, 120, 317, doi: 10.1086/533420

Osborn, W. 1971, The Observatory, 91, 223

Paxton, B., Bildsten, L., Dotter, A., et al. 2011, The Astrophysical Journal Supplement Series, 192, 3, doi: 10.1088/0067-0049/192/1/3

Piotto, G., Bedin, L. R., Anderson, J., et al. 2007, The Astrophysical Journal Letters, 661, L53, doi: 10.1086/518503

Plez, B. 2008, Physica Scripta Volume T, 133, 014003, doi: 10.1088/0031-8949/2008/T133/014003

Roh, D.-G., Lee, Y.-W., Joo, S.-J., et al. 2011, ApJL, 733, L45, doi: 10.1088/2041-8205/733/2/L45

Sandage, A. R. 1953, AJ, 58, 61, doi: 10.1086/106822

Seaton, M. J., Yan, Y., Mihalas, D., & Pradhan, A. K. 1994, MNRAS, 266, 805, doi: 10.1093/mnras/266.4.805

Sollima, A. 2019, Monthly Notices of the Royal Astronomical Society, 489, 2377, doi: 10.1093/mnras/stz2093

Stetson, P. B., & Harris, W. E. 1988, The Astronomical Journal, 96, 909, doi: 10.1086/114856

Tayar, J., Somers, G., Pinsonneault, M. H., et al. 2017, The Astrophysical Journal, 840, 17

van Saders, J. L., & Pinsonneault, M. H. 2012, ApJ, 751, 98, doi: 10.1088/0004-637X/751/2/98

Vinyoles, N., Serenelli, A. M., Villante, F. L., et al. 2017, The Astrophysical Journal, 835, 202